Langmuir Article
pubs.acs.org/Langmuir

Liquid Microdroplet Sliding on Hydrophobic Surfaces in the Presence of an Electric Field

Yuliang Wang[†,‡] and Bharat Bhushan*[,†]

[†]Nanoprobe Laboratory for Bio- & Nanotechnology and Biomimetics (NLB[2]), The Ohio State University, 201 West 19th Avenue, Columbus, Ohio 43210-1142, and [‡]Mechanical Engineering, Harbin Institute of Technology, Harbin 150001, P.R. China

Received September 14, 2009. Revised Manuscript Received September 29, 2009

Liquid droplet sliding is an approach for the transportation and manipulation of fluids in micro/nanofluidics related biosensor applications. Liquid droplet sliding is also instructive to evaluate the degree of boundary slip. In this study, liquid microdroplet sliding is studied with and without the presence of an electric field using atomic force microscopy on a polystyrene surface spin coated on a doped silicon wafer with a silicon oxide coating. Droplets with different diameters are slid with an atomic force microscope tip, and the sliding forces or lateral friction forces are quantitatively measured. Experimental results show that lateral friction force linearly increases with increasing droplet diameters, which can be explained by a droplet sliding model. When the electric field is applied, in addition to the decreased contact angle, diameters of the liquid droplets will increase. As a result, the electric field increases lateral friction force. To further investigate the impact of applied potential on lateral friction force, voltages from 0 to 80 V are applied to a droplet. Lateral friction force is found to increase with applied potential.

1. Introduction

The rapid development of micro/nanoscale fabrication techniques combined with biology and life science have stimulated the development of techniques for transportation and manipulation of fluids on the microscale.[1] One way to transport fluids is to slide liquid droplets over surfaces. Various techniques have been used to transport liquids as droplets by generating a gradient of wettability,[2-4] a driving force based on molecular absorption by selection of the molecular structure of the incorporated adsorbates,[5] or dielectrophoretic forces which attract polarizable objects to areas of high field intensity in an alternating or constant electric field.[6] On the microscale, surface forces, especially capillary forces, become dominant compared with the gravitational force and can be applied to micromanipulation by forming a liquid bridge between a probe and target objects.[7-10] Regarding droplet sliding, the capillary forces also play an important role through forming an unbalanced force between the front and back sides of the sliding droplets.[11,12]

In addition to the practical applications just mentioned, liquid droplet sliding is also instructive to evaluate the degree of boundary slip on hydrophobic and superhydrophobic surfaces of interest in micro/nanofluidics. It has been experimentally proven that boundary slip exists at the solid−liquid interface on both hydrophobic and superhydrophobic surfaces.[13-15] The existence of boundary slip can reduce drag in fluid flow, which is particularly meaningful in micro/nanofluidics. Regarding the mechanism of the boundary slip, nanobubbles[16-18] present at liquid−solid interfaces on hydrophobic and superhydrophobic surfaces are thought to be the reason.

In micro/nanofluidics based biosensor applications, polymers are widely used. The effect of surface charge to fluid flows on the micro/nanoscale is of interest to both droplet sliding and boundary slip studies. It is well-known that the wettability of conducting liquids on a dielectric layer between two electrodes can be controlled by applied electric field between the electrodes, which is called electrowetting.[19,20] The presence of an electric field reduces the surface tension between the liquid and the substrate, leading to a reduction of the contact angle and enhancing the wettability of the liquid.[21] Since the contact angle and surface tension of liquid droplets can be tuned locally with applied potentials, electrowetting has been intensively used to study sliding of fluid droplets with designed configuration of electrodes and switching of applied potentials.[22,23] Regarding boundary slip study, an electric field is expected to affect the fluid flow by changing the interaction between liquid and solid surfaces.

As mentioned earlier, although liquid droplet sliding has been achieved with various approaches, current research mainly

*Corresponding author. E-mail: Bhushan.2@osu.edu.
(1) Bhushan, B. *Springer Handbook of Nanotechnology*, 2nd ed.; Springer: Heidelberg, Germany, 2007.
(2) Chaudhury, M. K.; Whitesides, G. M. *Science* **1992**, *256*, 1539–1541.
(3) Ichimura, K.; Oh, S. K.; Nakagawa, M. *Science* **2000**, *288*, 1624–1626.
(4) Daniel, S.; Chaudhury, M. K.; Chen, J. C. *Science* **2001**, *291*, 633–636.
(5) Lee, S. W.; Laibinis, P. E. *J. Am. Chem. Soc*. **2000**, *122*, 5395–5396.
(6) Velev, O. D.; Prevo, B. G.; Bhatt, K. H. *Nature* **2003**, *426*, 515–516.
(7) Obata, K. J.; Motokado, T.; Saito, S.; Takahashi, K. *J. Fluid Mech*. **2004**, *498*, 113–121.
(8) Lambert, P.; Delchambre, A. *Assem. Autom*. **2005**, *25*, 275–283.
(9) Saito, S.; Motokado, T.; Obata, K. J.; Takahashi, K. *Appl. Phys. Lett*. **2005**, *87*, 234103.
(10) Bhushan, B.; Ling, X. *J. Colloid Interface Sci*. **2009**, *329*, 196–201.
(11) Furmidge, C. G. L. *J. Colloid Sci*. **1962**, *17*, 309–324.
(12) Roura, P.; Fort, J. *Langmuir* **2002**, *18*, 566–569.
(13) Maali, A.; Bhushan, B. *J. Phys.: Condens. Matter* **2008**, *20*, 315201.
(14) Bhushan, B.; Wang, Y.; Maali, A. *Langmuir* **2009**, *25*, 8117–8121.
(15) Wang, Y.; Bhushan, B.; Maali, A. *J. Vac. Sci. Technol., A* **2009**, *27*, 754–760.
(16) Bhushan, B.; Wang, Y.; Maali, A. *J. Phys.: Condens. Matter* **2008**, *20*, 485004.
(17) Wang, Y.; Bhushan, B.; Zhao, X. *Nanotechnology* **2009**, *20*, 045301.
(18) Wang, Y.; Bhushan, B.; Zhao, X. *Langmuir* **2009**, *25*, 9328–9336.
(19) Quilliet, C.; Berge, B. *Curr. Opin. Colloid Interface Sci*. **2001**, *6*, 34–39.
(20) Mugele, F.; Baret, J. C. *J. Phys.: Condens. Matter* **2005**, *17*, R705–R774.
(21) Bhushan, B.; Ling, X. *J. Phys.: Condens. Matter* **2008**, *20*, 485009.
(22) Pollack, M. G.; Fair, R. B.; Shenderov, A. D. *Appl. Phys. Lett*. **2000**, *77*, 1725–1726.
(23) Cho, S. K.; Moon, H. J.; Kim, C. J. *J. Microelectromech. Syst*. **2003**, *12*, 70–80.

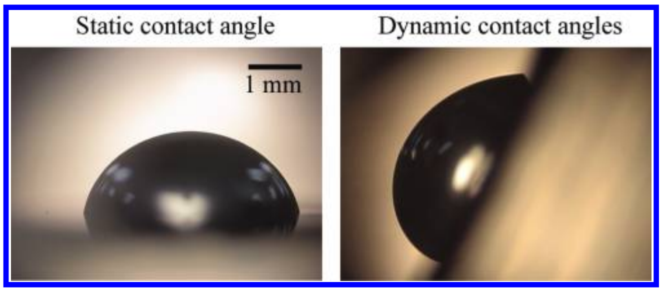

Figure 1. Images of a static (left) and a sliding glycerin droplet on an inclined (right) PS surface spin coated on SiO_2 substrate. Static and dynamic contact angles can then be measured from the profiles of the static and the moving droplets, respectively. Obtained static, advancing, and receding contact angles are 82.2°, 98.9°, and 60.3°, respectively.

focuses on realization of liquid motion, and the driving forces are seldom measured, especially when potentials are applied to the droplets and the substrate electrodes. The measurement of sliding forces is of significance for liquid manipulation related micro/nanofluidics applications. The measurement of sliding forces can provide evidence for the quantitative evaluation of the capability of liquid droplet sliding on specified surfaces. In this study, we have developed a new method to quantitatively measure the sliding force with an atomic force microscope (AFM) on hydrophobic surfaces. First, calibration for AFM lateral friction force is carried out. Then micromanipulation is carried out to line up microdroplets of different sizes by the AFM tip. The force needed to slide each droplet is measured. To study the effect of electric field on liquid droplet sliding, the sliding force is measured for each droplet with electric potentials applied between the AFM tip and sample surface. The impact of electric potential on droplet sliding is discussed.

2. Experimental Section

In this section, the experimental setup, sample preparation, and procedure of the experiment are first introduced. The detailed process of AFM lateral force calibration is then presented.

2.1. Experimental Setup and Procedure. The droplet sliding experiment was performed on a polystyrene (PS) surface spin coated on a p-type boron doped silicon wafer (1−20 Ω cm, Silicon Quest International) with a 300 nm thick silicon oxide coating thermally grown on the wafer. The silicon oxide wafer was first cleaned in a sonication bath of acetone and then water before spin coating. PS (molecular weight 350 000, Sigma-Aldrich) particles were dissolved in toluene solution with a concentration of 1.5% (weight). The PS solution was then spin coated onto the silicon oxide wafer at a speed of 500 rpm. The thickness of the coated PS film was measured to be about 60 nm with an ellipsometer (model L116C, Gaertner Scientific Corporation). After that, the PS surface was glued to a metal AFM sample plate with conductive silver paint to make sure the doped silicon substrate and the sample plate are electrically connected.

The droplet sliding experiment was performed with a commercial AFM (Dimension 3000, Veeco). An n-type silicon (0.5−2 Ω cm) cantilever with a nominal spring constant of 3 N/m and tip radius of less than 10 nm was used to slide liquid droplets. The liquid is the mixture of water, glycerin, and sodium chloride (NaCl). The glycerin was added to keep droplets from evaporating in the ambient environment, whereas the NaCl was added to make the liquid conductive to perform electrowetting experiments. The static contact angle was measured with a sessile drop method, as shown in Figure 1 (left). To measure the dynamic contact angle, the glycerin drop was put on a inclined PS surface. The incline angle was gradually increased until the liquid drop started to slide, and then the image was taken, as shown in Figure 1 (right). The advancing and receding contact angles measured on the sliding profile at lower contact line and upper contact are 98.9 ± 2.3° and 60.3 ± 1.7°, respectively.

Before performing the droplet sliding experiment, the AFM cantilever was first used to laterally scan on a silicon (100) substrate to calibrate lateral friction force. The conversion factor which converts lateral deflection signal to friction force was obtained. To deposit small droplets and then conduct the droplet sliding experiment, a small amount of liquid mixed with a large amount of air was quickly sprayed on the PS sample.[21] Droplets with diameters of less than 100 μm were obtained on the surface. Before sliding, the relative positions between the cantilever tip and target liquid droplets were adjusted by changing the positions of the sample stage with the integrated function of the Dimension AFM. After that, droplets of different sizes were first lined up through cantilever tip manipulation and then slid by the cantilever tip. The sliding speed was 100 μm/s. Here, one should make sure all liquid in a droplet slides with the cantilever tip, otherwise the friction force will be underestimated due to the decreased size of the droplets. By optical microscopy observation, we find this is satisfied on the PS surface used in this study, and the PS surface remains dry after droplets slide over. To investigate the impact of applied potentials on droplet sliding, applied potentials in the range of 0−80 V were applied between the cantilever tip and the sample substrate using a DC power supply (E3612A, HP), and the sample substrate was connected to power supply ground.

2.2. Lateral Friction Force Calibration. During sliding, the cantilever lateral deflection signal was obtained. To convert the lateral deflection into lateral friction force, it is necessary to calibrate the lateral friction force for the experimental setup used. Generally, AFM lateral force can be calibrated with a parallel scan method,[24,25] a wedge method,[26] or a method relying on stick contact between the cantilever tip and sample surface before relative motion occurs.[27] In this study, we call it the pivot method. Here, the lateral friction force generated during droplet sliding is calibrated with the pivot method.

When the cantilever tip laterally slides on a sample surface, the cantilever and the contact can be taken as two springs in series. Therefore, the total lateral contact stiffness k_{tot} can be given as

$$k_{tot} = \left[\frac{1}{k_{cant}} + \frac{1}{k_{contact}}\right]^{-1} \quad (1)$$

where k_{cant} and $k_{contact}$ are the lateral spring constant and lateral contact stiffness, respectively. For the cantilever used in this study, k_{cant} is approximately 364 N/m with the cantilever dimensions and material properties (elastic modulus 130 GPa and Poisson's ratio 0.28).[28,29] The lateral contact stiffness $k_{contact}$ is given by[30]

$$k_{contact} = 8G^*a \quad (2)$$

where $G^* = [(2-\nu_1)/G_1 + (2-\nu_2)/G_2)]^{-1}$, and the radius a of the contact area is given as

$$a = \left(\frac{3RF_z}{4E^*}\right)^{1/3} \quad (3)$$

where R is the tip radius, F_z is the normal load, and $E^* = [(1-\nu_1^2)/E_1 + (1-\nu_2^2)/E_2]$.[31] In the above equations, G_1 and G_2 are

(24) Ruan, J. A.; Bhushan, B. *J. Tribol.* **1994**, *116*, 378–388.
(25) Wang, Y.; Zhao, X.; Zhou, F. *Rev. Sci. Instrum.* **2007**, *78*, 036107.
(26) Ogletree, D. F.; Carpick, R. W.; Salmeron, M. *Rev. Sci. Instrum.* **1996**, *67*, 3298–3306.
(27) Cain, R. G.; Biggs, S.; Page, N. W. *J. Colloid Interface Sci.* **2000**, *227*, 55–65.
(28) Anonymous. *Properties of Silicon*; EMIS data reviews series No. 4. INSPEC; Institution of Electrical Engineers: London, 1988.
(29) Bhushan, B.; Ling, X. *J. Phys.: Condens. Matter* **2008**, *20*, 485009.
(30) Singer, I. L.; Pollock, H. M. *Fundamentals of Friction: Macroscopic and Microscopic Processes*; Kluwer Academic: Dordrecht, 1992; p 111.
(31) Bhushan, B. *Introduction to Tribology*; Wiley: New York, 2002.

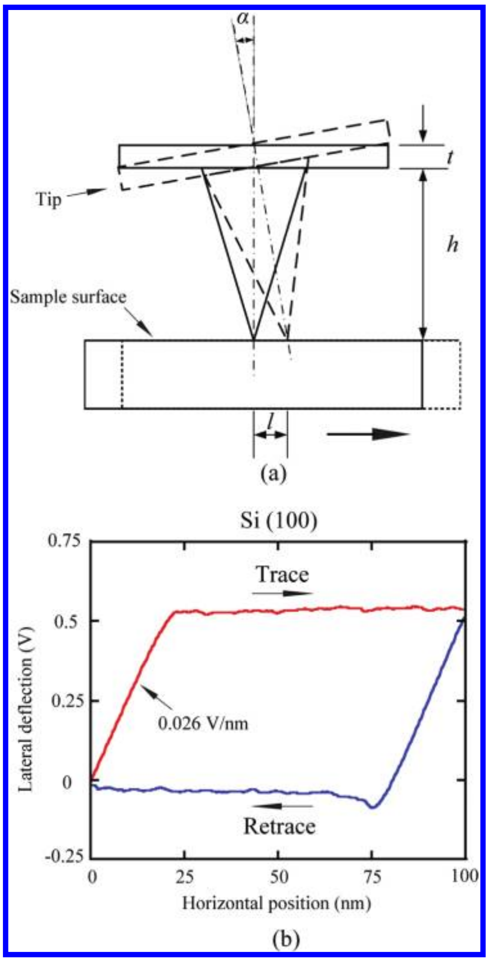

Figure 2. (a) Schematic of cantilever deformation induced by small lateral displacement l of the sample surface. Solid and dashed features represent the tip and sample surface before and after lateral displacement l, respectively. h and t are tip height and thickness of the cantilever, respectively. Twist angle α is generated. (b) AFM friction loop of the silicon cantilever on a silicon (100) substrate. Slopes at the beginning of the trace and retrace motions represent the stick contact between the AFM tip and the Si substrate. The slope value of 0.026 V/nm is then used to calibrate lateral deflection signal of the cantilever.

shear moduli, E_1 and E_2 are elastic moduli, and ν_1 and ν_2 are Poisson's ratio for the tip and sample surface, respectively. Because both the tip and sample surface are silicon, taking $E_1 = E_2 = 130$ GPa, $\nu = 0.28$, applied normal load $F_z = 300$ nN, and tip radius $R = 10$ nm, the lateral contact stiffness is approximately 375×10^6 N/m, which is much larger than k_{cant}. From eq 1, it is clear that $k_{tot} \approx k_{cant}$, which means the deflection mainly occurs in the cantilever.

When the condition $k_{tot} \approx k_{cant}$ is satisfied, as in this study, the principle of the pivot method for lateral friction force calibration can be demonstrated in Figure 2a. The solid and dashed features represent the cantilever and sample surface before and after a small lateral displacement l of the sample surface, respectively. Since l is small, the tip sticks on the sample surface due to the static friction force generated by applied normal load and adhesion force. Therefore, there is no relative movement between the tip and the sample surface.

Figure 2b shows a friction loop obtained based on 10 measurements with a scan size 100 nm and scan rate 1 Hz. It is very clear that, at the beginning of trace and retrace motions, the lateral deflection signal linearly increases with horizontal position. The slope value C_{slope} is about 0.026×10^9 V/m. During lateral scanning, the lateral friction force F_f applied to the tip is proportional to the lateral deflection signal $V_{lateral}$ and can be given as

$$F_f = CV_{lateral} \tag{4}$$

where C is the conversion factor which converts the lateral deflection signal to F_f. From Figure 2b, one can see that $V_{lateral}$ can be given as

$$V_{lateral} = C_{slope} l \tag{5}$$

The lateral friction force F_f exerted on the cantilever tip because of displacement l can also be given as

$$F_f = lk_{cant} = l\frac{k_\alpha}{(h+t/2)^2} \tag{6}$$

where $k_\alpha = Ewt^3/6L(1 + \nu)$ is the torsional stiffness of the cantilever. By combining eqs 4−6, the conversion factor C is then obtained as

$$C = \frac{k_\alpha}{C_{slope}(h+t/2)^2} \tag{7}$$

By inserting corresponding values into eq 7, the conversion factor of about 1.40×10^4 nN/V is obtained. During the experiment, there is a separation d between the bottom of the tip and the sample surface, and it was kept as 3 μm to make the conversion factor constant during experiments. Therefore, the conversion factor C needs to be adjusted because of the existence of d as $C_{sliding} = C(h + t/2)^2/(h + t/2 + d)^2 = 1.05 \times 10^4$ nN/V.

3. Results and Discussion

In this section, microsized droplets with different diameters will be slid with and without applied potentials, followed by an investigation of the impact of applied potentials on the sliding of a certain size droplet.

3.1. Impact of Electrowetting on Microdroplets. Figure 3a left and right shows a liquid droplet before and after the potentials are applied between the tip and the substrate, respectively. θ_Y and θ_V, w_1 and w_2 are the static contact angles and width of the droplet before and after the potential V is applied, respectively, and d is the separation distance between the bottom of the cantilever tip and the sample surface of the PS film.

The presence of V reduces surface tension and hence reduces the static contact angle. When V is applied between the droplet and doped silicon substrate, the contact angle θ_V of the droplet can be expressed by the so-called Lippmann equation,[20]

$$\cos\theta_V = \cos\theta_Y + \frac{\varepsilon_0\varepsilon_d}{2t_d\gamma_{LV}}V^2 \tag{8}$$

where θ_Y is the Young's contact angle, ε_0 and ε_d are the dielectric constants of the vacuum and insulator, respectively, t_d is the thickness of the insulator, and γ_{LV} is the interfacial tension of the liquid.

In addition to the decrease of contact angle demonstrated in Figure 3a, the width of the droplet is expected to increase due to the decrease of the contact angle. To verify the change of the width, the cantilever is first attached to a droplet with a diameter of about 60 μm, as shown in Figure 3b. Then voltages of 20 and 40 V are applied. It is clear that the size of the droplet increases with applied potentials. From eq 8, one can see that, in addition to electric potential V, the thickness t_d also influences the variation of contact angle. When the thickness decreases, the contact angle will further decrease. As a consequence, the width of the droplets will increase.

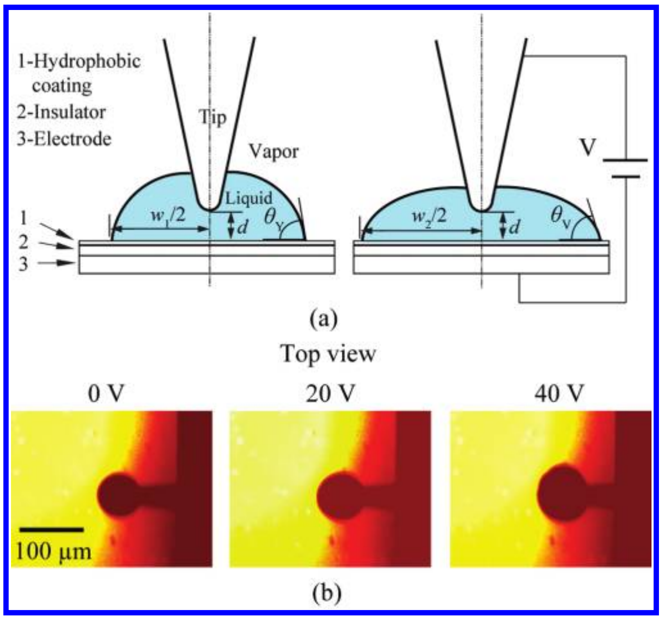

Figure 3. (a) Schematic of a liquid droplet without (left) and with (right) an applied potential V. Before applying V, the contact angle is θ_Y with a diameter of w_1. When V is applied, the contact angle decreases to θ_V and the diameter of the droplet increases to w_2. During the experiment, the distance d between the bottom of the tip and the sample surface is kept as 3 μm. (b) Top view of a droplet attached by the AFM cantilever with different applied potentials. The diameter increases with increasing potentials.

3.2. Sliding of Droplets with Different Size. Regarding liquid droplet sliding, Furmidge[11] derived an equation describing the relationship between contact angle hysteresis and the sliding angle of a water droplet on a slope. This relationship is widely used to study the movement and manipulation of water droplets.[12] The sliding angle is the angle of tilted surface necessary to produce droplet sliding. Figure 4 shows a droplet during sliding along a slope. The dashed and solid profiles represent the droplet before and after movement, respectively. When the droplet slides downward, the distance dl along the slope with inclined angle ϕ without acceleration, the work W done by the drop due to the component of weight along the slope can be given as

$$W = mg \sin \phi dl \tag{9}$$

where m is the mass of the drop and g is the acceleration of gravity. The work done by the drop in moving a distance dl can be given as[11]

$$W = \gamma_{LV} w dl \cos \theta_{rec} - \gamma_{LV} w dl \cos \theta_{adv} \tag{10}$$

where γ_{LV} is the liquid vapor surface tension and w is the width of the droplet along the direction perpendicular to the direction of droplet movement. By combining eqs 9 and 10, one can get the relationship between the sliding angle needed to make the droplet move downward and the advancing and receding contact angles, given as[11]

$$mg \sin \phi = \gamma_{LV} w(\cos \theta_{rec} - \cos \theta_{adv}) \tag{11}$$

In this case, the driving force to slide droplets is provided by the cantilever tip, and not by gravity. Figure 5 shows schematically a droplet sliding without (left) and with (right) an applied potential. During sliding, the front side and back side contact angles of the

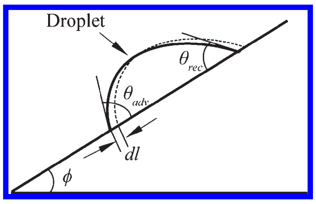

Figure 4. Schematic of a droplet sliding downward along a slope without acceleration. The dashed and solid profiles separately represent the droplet before and after the displacement dl down the slope, respectively.

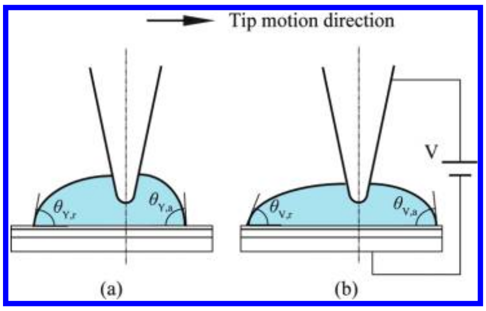

Figure 5. Schematic of a liquid droplet sliding by the motion of the AFM tip without (left) and with (right) the potential V. $\theta_{Y,a}$ and $\theta_{Y,r}$ are advancing and receding contact angles without V, while $\theta_{V,a}$ and $\theta_{V,r}$ are advancing and receding contact angles with V, respectively.

droplet are expected to be the advancing and receding contact angles of the droplet.[12] Therefore, the angles $\theta_{Y,a}$, $\theta_{V,a}$ and $\theta_{Y,r}$, $\theta_{V,r}$ are advancing and receding contact angles for the droplet without and with the applied potential, respectively.

The immersion of an AFM tip into the droplet may change the profile of the droplet, which will further change the width of the droplet. Therefore, it is necessary to check the portion of the AFM tip immersed in the liquid droplet. According to the geometry of the cantilever tip used in our study and experimental setup, the volume of the cantilever tip immersed in the liquid droplet takes less than 5% of the liquid droplet volume for each droplet. Therefore, the width of the droplet before immersion of the cantilever tip can be approximately taken as the value during liquid droplet sliding. According to eq 11, the initial forces $F_{Y,init}$ and $F_{V,init}$ needed to drive the droplet without and with the applied potential can be separately given as

$$F_{Y,\,init} = \gamma_{LV} w_1(\cos \theta_{Y,\,r} - \cos \theta_{Y,\,a}) \tag{12}$$

$$F_{V,\,init} = \gamma_{LV} w_2(\cos \theta_{V,\,r} - \cos \theta_{V,\,a}) \tag{13}$$

Due to the presence of applied potential V, w_2 is larger than w_1. Therefore, the presence of V is expected to increase initial force, namely $F_{V,init} > F_{Y,init}$.

Four droplets with diameters of less than 30 μm are slid in this study, as shown in the inset image of Figure 6. The droplets were first lined up in a sequence of increasing size. Then they were separately slid without applied potentials. After that, 20 V potential was applied between the tip and the substrate. The lateral friction force for droplets without and with the 20 V potential are plotted in Figure 6. Without the potential, friction force linearly increases with droplet diameters, as indicated by eq 12. After the 20 V potential is applied, the friction force also increases with increasing droplet diameter. More importantly, the applied potential greatly increases the friction force for each

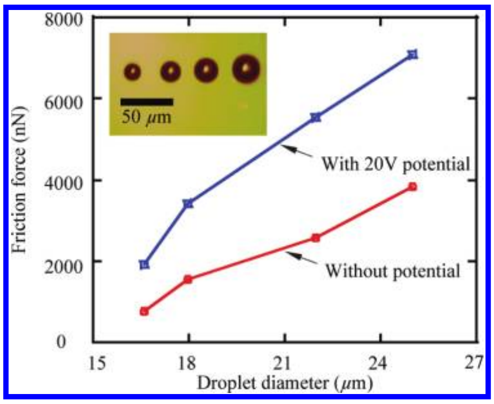

Figure 6. Friction force as a function of droplet diameter with and without 20 V potential when droplets are slid by the cantilever tip. Friction force increases with droplet size as well as with the applied potential. The inset shows an optical image of droplets with different sizes.

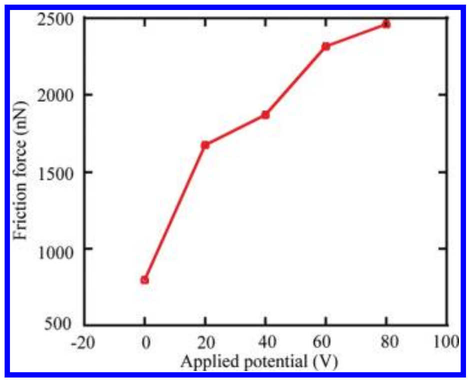

Figure 7. Friction force as a function of applied potential. Friction force increases with applied potentials.

droplet. To further investigate the impact of applied potentials on lateral friction force, different potentials were applied to a droplet with a diameter of about 16.5 μm. The friction force as a function of applied potentials is plotted in Figure 7. Friction forces are also found to increase with applied potentials. The phenomenon of increased friction force with applied potentials is consistent with the increasing diameter of droplets induced by the applied potentials as shown in Figure 3b. As mentioned earlier, since the thickness of the insulator will change the contact angle and hence the width of the droplets, in addition to an applied electric field, one can also change the sliding force through adjusting the thickness of the coating. By decreasing the thickness, the sliding force can further be increased.

4. Conclusions

Liquid microdroplet sliding is studied without and with the presence of an electric field using atomic force microscopy on a polystyrene surface spin coated on a doped silicon wafer with a silicon oxide coating. Droplets of different diameters are slid with an AFM tip, and the sliding forces, which are called lateral friction force, are quantitatively measured. The lateral friction forces are found to linearly increase with droplet diameters. That is because the sliding force is proportional to the diameter of the droplets based on a model. In addition to the decreased contact angle, the presence of applied potentials increases the diameter of droplets. When a 20 V potential is applied between the cantilever tip and the substrate, the obtained lateral friction force also increases with increasing droplet diameter. More importantly, the friction force with the applied potential is larger than that without the potential for each droplet, because the applied potential increases droplet size. To further investigate the impact of applied potentials on lateral friction force, voltages from 0 to 80 V are applied to a certain droplet. Lateral friction force is found to increase with applied potential.

Acknowledgment. Y.W. acknowledges financial support from Chinese Scholarship Council.